SeiSIM: Structural Similarity Evaluation for Seismic Data Retrieval

Zhiling Long, Zhen Wang, and Ghassan AlRegib
Center for Energy and Geo Processing (CeGP) at Georgia Tech and King Fahd University of Petroleum and Minerals (KFUPM)
School of Electrical and Computer Engineering
Georgia Institute of Technology
Atlanta, Georgia 30332, USA
Email: {zhiling.long, zwang313, alregib}@gatech.edu

***Abstract*—Structural similarity evaluation is a critical step for retrieving existing databases to find matching records for a given seismic data set. The objective is to enable the re-use of historical findings to assist exploration with new survey data. Currently there are very few structural similarity metrics specifically designed for seismic data, especially seismic survey maps. In this paper, we propose a metric that combines texture similarity and geological similarity, which is derived from discontinuity maps. We test the seismic similarity metric in a retrieval application. The successful results indicate that our approach is promising.**

I. Introduction

With the existence of a large amount of seismic databases established over the years, it will be profitable if the associated historical findings may be re-used to assist exploration with new survey data. To accomplish this, it is necessary to retrieve the historical data sets and identify the ones with seismic structures similar to those of the new data set of interest. Thus, suitable metrics are in need to evaluate structural similarity between seismic data sets. Figure 1 illustrates this retrieval problem.

To investigate this problem, we start with a simple form of seismic survey data, i.e., 2-D survey maps (which is simply denoted as seismic images in this paper when there is no confusion). A few similarity metrics were proposed in recent years for various seismic applications. For example, in [1] a method was proposed based on the singular value decomposition of acoustic echo envelopes for seabed sediments classification. In [2] similarity of curves was examined for clustering of seismic waveforms. Since both techniques involve data of forms totally different than survey maps, they may not be applicable to our study. In [3] it was suggested to use attributes such as cross correlation and semblance as similarity metrics for identification of relevant data volumes during stacking. The emphasis was on identifying data sets that belong to the same location, rather than locations of similar geological structures. Thus, it may not be suitable for us due to more constraints placed upon the solution.

Structural similarity evaluation for visual images, or images of natural scenes, has been advancing rapidly in the past decade. Among various techniques, SSIM (Structural SIMilarity) [4] and its several extensions have been widely accepted as useful metrics that capture structural visual characteristics.

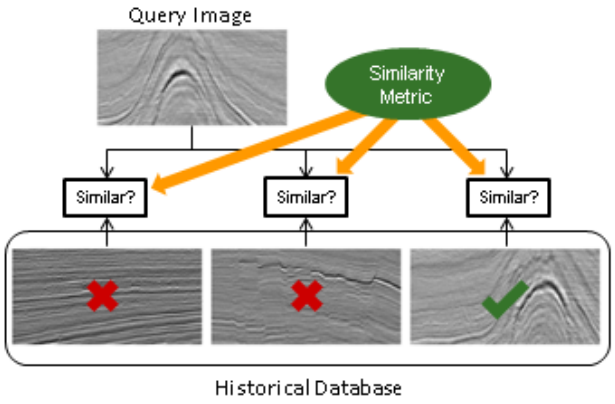

Fig. 1. Illustration of the seismic retrieval problem.

However, these techniques may not necessarily be applicable to seismic images. Instead of recording natural scenes, seismic images are synthetically generated, with unique visual appearance representing various geological structures such as horizons, faults, salt domes, etc.

Typically, seismic images are textural in nature. As such, it may be expected that similarity metrics developed for texture images would fit better for the intended seismic applications. Although this idea seems reasonable, currently available texture similarity metrics [5] are still aimed towards visual images. We believe that, for seismic images, geological attributes associated with the typical structures ought to be reflected in such objective metrics. Therefore, suitable similarity assessment methods specifically for seismic images need to be developed.

In this paper, we propose a metric for seismic similarity evaluation. Based on the aforementioned observation that seismic images resemble texture images in appearance, we establish our development on available texture similarity metrics. To incorporate geological information, we utilize a discontinuity map generated from seismic images, and combine the derived geological similarity with texture similarity into the seismic similarity. We test our design on a small-scale seismic retrieval application.

978-1-4799-6532-8/15/$31.00

II. Methods

A. Structural Visual Similarity

The SSIM index [4] has been widely accepted as an effective measure for structural comparison of visual images. Assuming two signals **x** and **y**, the SSIM between the signals is calculated as

$$SSIM\left(\mathbf{x},\mathbf{y}\right)=\left[l\left(\mathbf{x},\mathbf{y}\right)\right]^{\alpha}\left[c\left(\mathbf{x},\mathbf{y}\right)\right]^{\beta}\left[s\left(\mathbf{x},\mathbf{y}\right)\right]^{\gamma} \tag{1}$$

where α, β, and γ are parameters for adjusting the relative importance of the three associated components, i.e., differences in luminance, contrast, and structure, as calculated below.

$$l(\mathbf{x},\mathbf{y})=\frac{2\mu_x\mu_y+C_l}{\mu_x^2+\mu_y^2+C_l} \tag{2}$$

$$c(\mathbf{x},\mathbf{y})=\frac{2\sigma_x\sigma_y+C_c}{\sigma_x^2+\sigma_y^2+C_c} \tag{3}$$

$$s(\mathbf{x},\mathbf{y})=\frac{\sigma_{xy}+C_s}{\sigma_x\sigma_y+C_s} \tag{4}$$

Here, μ_x and μ_y are the mean intensities; σ_x and σ_y are the standard deviations; σ_{xy} is the covariance between the two signals; and C_l, C_c and C_s are constants associated with the dynamic range of the signals. When α, β, and γ are all set to 1, the simplified expression for SSIM becomes

$$SSIM\left(\mathbf{x},\mathbf{y}\right)=\frac{\left(2\mu_x\mu_y+C_1\right)\left(2\sigma_{xy}+C_2\right)}{\left(\mu_x^2+\mu_y^2+C_1\right)\left(\sigma_x^2+\sigma_y^2+C_2\right)} \tag{5}$$

where C_1 and C_2 are constants similar to C_l, C_c and C_s above.

Since the introduction of SSIM, several improved versions have been proposed in the literature. For example, MS-SSIM [6] applies a multiscale decomposition to the images involved in the evaluation, and calculates the index within each scale before integrating them together. MS-SSIM provides more flexibility regarding the variations of image resolution and viewing conditions and it adopts to the human visual system. CW-SSIM [7] performs the SSIM-like assessment in the complex wavelet domain to reduce the impact of translation, rotation, or scaling of the images. Most recently, IW-SSIM [8] was developed to incorporate a weighting scheme that is based on the information content of the images.

B. Structural Texture Similarity

Although SSIM and its variants are useful metrics for visual image structural similarity, their structural comparison is still based on point-to-point cross correlation between two images. As [9] pointed out, this makes it inappropriate for texture images, where two texture images may be perceived as from the same pattern yet with significant point-to-point variance. To tackle this problem, a group of structural texture similarity (STSIM) metrics were proposed by [9]. Such metrics employ completely area based statistics to avoid point-to-point correspondence.

STSIM metrics are established on the basis of a multiresolution image decomposition framework, i.e., the steerable pyramid representation developed by [10]. As illustrated in Figure 2, the technique first decomposes a given image into a highpass subband (sub-image) and a lowpass subband. Then it processes the lowpass subband, obtaining a series of bandpass subbands and another lowpass subband. The bandpass subbands reveal image details along various orientations. The newly obtained lowpass subband is subsampled and then further processed in a similar manner to yield orientational details at a coarser spatial scale. Such recursive decomposition eventually yields a series of subbands, representing the original image along different orientations at different scales.

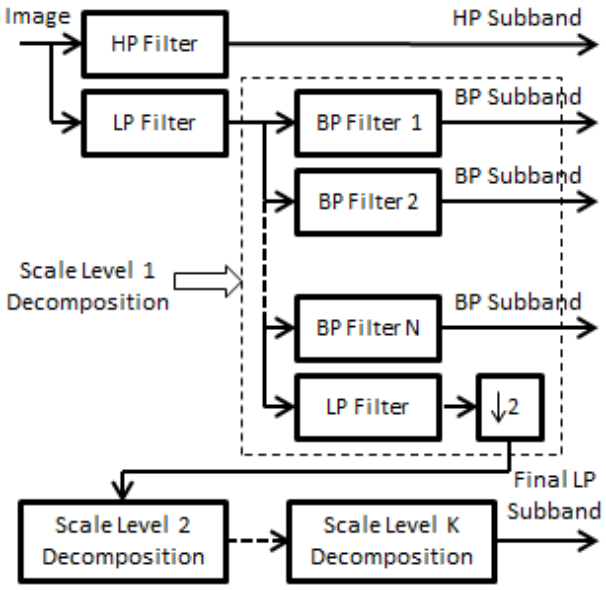

Fig. 2. Illustration of the steerable pyramid decomposition. In this example, it consists of K scales and N orientations at each scale.

STSIM metrics examine the subband images generated from a steerable pyramid decomposition. They calculate area based statistics within each subband and/or between subbands that are closely related in scale or orientation. As an initial effort, in this paper, we only explore with one of such metrics, that is, STSIM-1 [9]. As we will see in the experiments, this metric fits well for the seismic applications even though it is not the most sophisticated in the STSIM family.

STSIM-1 calculates for each decomposed subband three terms, namely, a luminance term, a contrast term, and a structure term. Obviously, this follows the concept inherent in SSIM. The difference lies in the structure term. Instead of examining the cross correlation between two images, STSIM-1 compares subband images with regard to two autocorrelation values. One is the horizontal autocorrelation, computed along each row. The other is the vertical autocorrelation, calculated along each column. The three terms are combined to yield a similarity score between subbands from two images, which are of the same scale and orientation. The overall similarity score is an average over all subbands from the pyramidal decomposition.

For a given $N\times M$ subband $\mathbf{x}(i,j), i=1,...,N, j=1,...,M$, the horizontal autocorrelation $\rho_{\mathbf{x}}^{h}$ is calculated as

$$\rho_{\mathbf{x}}^{h}=\frac{\mathbf{E}\{[\mathbf{x}(i,j)-\mu_x][\mathbf{x}(i,j+1)-\mu_x]^*\}}{\sigma_x^2} \tag{6}$$

and the vertical autocorrelation $\rho^v_{\mathbf{x}}$ is calculated as

$$\rho^v_{\mathbf{x}} = \frac{\mathbf{E}\{[\mathbf{x}(i,j) - \mu_x][\mathbf{x}(i+1,j) - \mu_x]^*\}}{\sigma_x^2} \tag{7}$$

Here, $\mathbf{E}(\cdot)$ refers to calculating the mean, and $*$ denotes the complex conjugate to accommodate complex steerable pyramid decomposition. The corresponding structure similarity terms comparing subbands $\mathbf{x}$ and $\mathbf{y}$ are computed as

$$a_h(\mathbf{x},\mathbf{y}) = 1 - 0.5|\rho^h_{\mathbf{x}} - \rho^h_{\mathbf{y}}|^p \tag{8}$$

and

$$a_v(\mathbf{x},\mathbf{y}) = 1 - 0.5|\rho^v_{\mathbf{x}} - \rho^v_{\mathbf{y}}|^p \tag{9}$$

where p is usually set to 1. Hence, the similarity score between the two subbands are computed as follows.

$$Q_{STSIM-1}(\mathbf{x},\mathbf{y}) = [l(\mathbf{x},\mathbf{y})]^{\frac{1}{4}}[c(\mathbf{x},\mathbf{y})]^{\frac{1}{4}}[a_h(\mathbf{x},\mathbf{y})]^{\frac{1}{4}}[a_v(\mathbf{x},\mathbf{y})]^{\frac{1}{4}} \tag{10}$$

where $l(\mathbf{x},\mathbf{y})$ and $c(\mathbf{x},\mathbf{y})$ are the luminance and contrast terms, respectively, as defined by the SSIM metric.

C. Geological Similarity

Discontinuity in horizons is one of the most prominent geological attributes, which is typically associated with faults. To measure the seismic discontinuity, we calculate the semblance attribute proposed by [11], which is accurate and robust by involving structural dips and neighboring average. According to the definition of semblance attribute, every point in a seismic section corresponds to a square analysis window with the size of $2r+1$, oriented parallel to local horizons. Therefore, the discontinuity value derived from the semblance attribute is calculated in the analysis window as:

$$D(x,z) = \left| \ln \left[\frac{\sum_{j=-r}^{r} \left(\sum_{i=-r}^{r} S(x+i, z+j) \right)^2}{(2r+1) \sum_{i=-r}^{r} \sum_{j=-r}^{r} S(x+i, z+j)^2} \right] \right|, \tag{11}$$

where x and z respectively correspond to crossline and depth direction. $S(x,z)$ represents the intensity of the seismic signal at (x,z) and the $\ln(\cdot)$ increases the discontinuity contrast between faults and horizons. A greater discontinuity value suggests a higher possibility of the point being located in faults, in contrast to $D(x,z)$ closing to 0 which indicates the point belongs to a horizon.

By calculating discontinuity for every point in an image, a discontinuity map (DM) can be obtained (see Figure 3 for examples). To determine the similarity between two discontinuity maps, we compute the horizontal autocorrelation ρ^h_{DM} and vertical autocorrelation ρ^v_{DM} for each map. Then we compare them by using a^h_{DM} and a^v_{DM} respectively, as shown below. Essentially, the calculation is very similar to what is done with STSIM-1. The difference here is that, now the calculation is conducted directly with the map values without going through the steerable pyramid decomposition.

$$\rho^h_{DM} = \frac{\mathbf{E}\{[DM(i,j) - \mu_{DM}][DM(i,j+1) - \mu_{DM}]^*\}}{\sigma^2_{DM}} \tag{12}$$

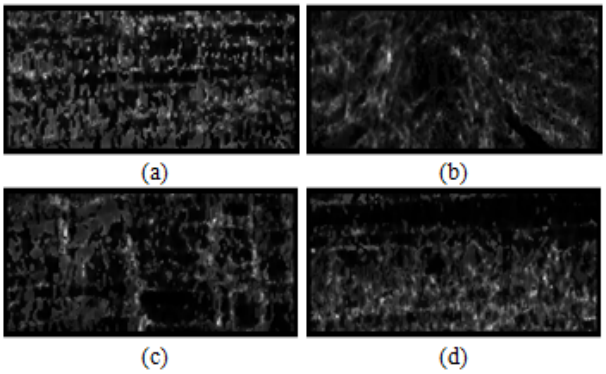

Fig. 3. Example discontinuity maps generated for each image group in the experimental data set in this study: (a) horizons; (b) salts; (c) faults; and (d) noisy horizons.

$$\rho^v_{DM} = \frac{\mathbf{E}\{[DM(i,j) - \mu_{DM}][DM(i+1,j) - \mu_{DM}]^*\}}{\sigma^2_{DM}} \tag{13}$$

$$a^h_{DM}(DM_1, DM_2) = 1 - 0.5|\rho^h_{DM_1} - \rho^h_{DM_2}| \tag{14}$$

$$a^v_{DM}(DM_1, DM_2) = 1 - 0.5|\rho^v_{DM_1} - \rho^v_{DM_2}| \tag{15}$$

The similarity score between two discontinuity maps DM_1 and DM_2 is then defined as

$$Q_{DM} = [a^h_{DM}(DM_1, DM_2)]^{\frac{1}{2}}[a^v_{DM}(DM_1, DM_2)]^{\frac{1}{2}} \tag{16}$$

D. Seismic Similarity (SeiSIM)

We combine texture similarity (STSIM-1) and geological similarity (DM) to generate our seismic similarity metric, which we denote as SeiSIM. As discussed earlier, texture similarity is expected to help differentiate between seismic images due to the textural appearance of seismic images. We expect that the incorporation of discontinuity map-based geological similarity will assist the further differentiation between seismic structures of similar textural appearance (e.g., horizons and faults). Consequently, the seismic similarity metric is expressed as

$$SeiSIM = [Q_{STSIM-1}]^{\frac{1}{2}}[Q_{DM}]^{\frac{1}{2}}. \tag{17}$$

III. Experiments

We test our seismic similarity metric in a simple image retrieval application. This section discusses the data sets we use, the retrieval performance evaluation methods, and the retrieval performance of different metrics.

A. Data

We created a small data set for preliminary experimentation. The data set consists of 4 types of seismic structures, each including 3 different images. The types are horizons, salts, faults, and noisy horizons. Figure 4 shows all 12 images in the data set. The images are of gray scale, 100×200 pixels each. They were all extracted from the Netherlands offshore F3 block acquired in the North Sea (available at https://opendtect.org/osr/).

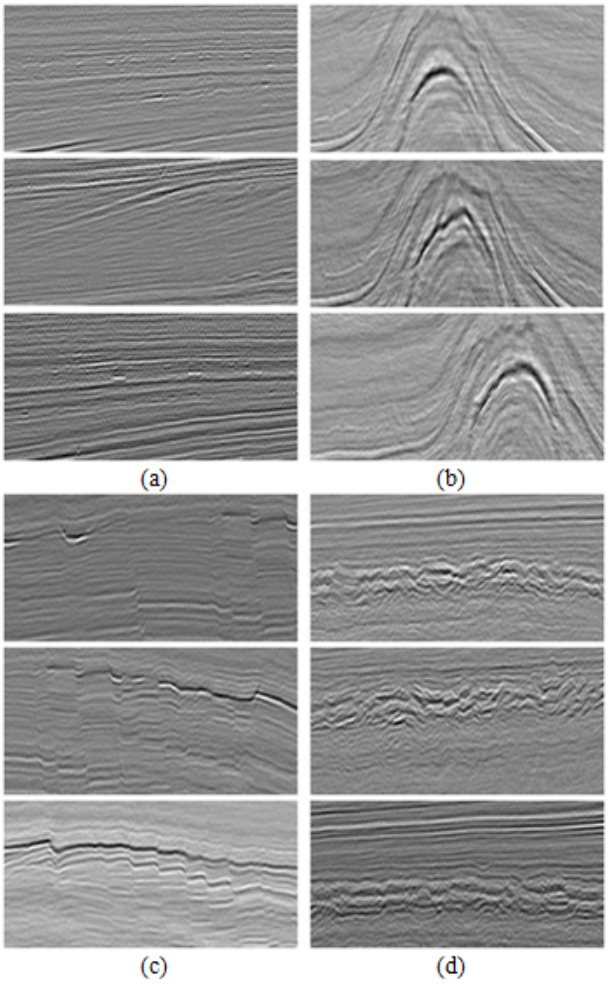

Fig. 4. Image groups used in the experiments (each group consists of three images of the same geological structure): (a) horizons; (b) salts; (c) faults; and (d) noisy horizons.

B. Performance Evaluation

The retrieval performance is typically evaluated by the following three measures [9]. They are all in the range of $0-1$, with the higher value indicating better performance.

- **Precision at one (P@1)**
  This index presents the frequency when the first image being retrieved has the same label as the query image, or matches the query.
- **Mean reciprocal rank (MRR)**
  This is the average inverse rank for the first matching image found in the database. The inverse rank is used so that a higher MRR value is for a better performance.
- **Mean average precision (MAP)**
  This index accounts for the case when multiple matching images are in existence in the database. For each query image, the database is retrieved till the last matching image is identified. For a certain matching image of which the rank is n, the fraction of total matching images among the first n retrieved images is used as the associated precision. The average retrieval precision for a query is calculated using the precision associated with each of its matching images. Then, the MAP is obtained by averaging across all query images.

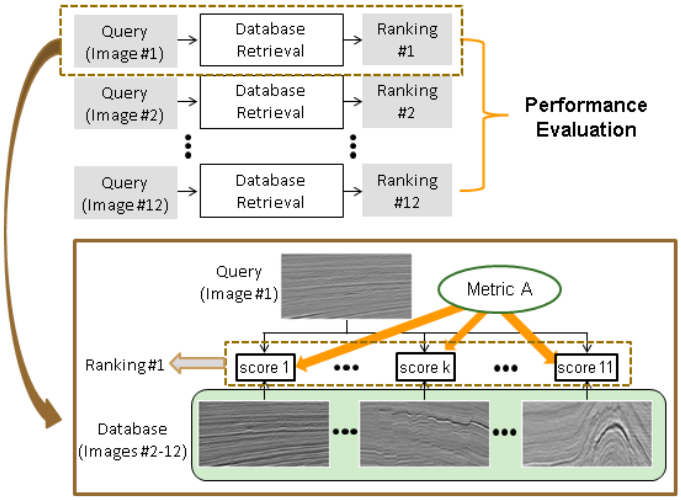

Fig. 5. Illustration of the procedure for the experiments.

TABLE I. RETRIEVAL PERFORMANCE USING DIFFERENT SIMILARITY METRICS.

Metric	P@1	MRR	MAP
SSIM	0.33	0.73	0.46
CW-SSIM	0.67	0.94	0.72
STSIM-1	0.92	0.99	0.91
DM	0.50	0.88	0.65
CW-SSIM + DM	0.92	0.97	0.82
STSIM-1 + DM (SeiSIM)	**1.00**	**1.00**	**0.97**

C. Results

We conducted retrieval experiments on the database using various similarity metrics discussed above. For each metric, every seismic image in the database was selected once as the query image. It was then compared with the rest 11 images, ranking them according to the similarity score in a descending order. Such ranking was obtained for all 12 images. Then the three performance values were assessed using the 12 rankings. The procedure is illustrated in Figure 5.

The metrics being examined were SSIM, CW-SSIM, STSIM-1, DM, CW-SSIM+DM, and STSIM-1+DM (i.e., SeiSIM). As discussed earlier, both CW-SSIM and STSIM-1 utilize the steerable pyramid decomposition to obtain a series of subbands describing the original seismic image at multiple scales and orientations. In all the experiments, we set the number of scales to be 4, and the number of orientations at each scale to be 8. Both SSIM and CW-SSIM indices are calculated based on local windows. The sliding window size was set to 7×7 according to the common practice in the literature. The retrieval performance with each respective similarity metric is summarized in Table I.

From Table I, it can be observed that SSIM performance is the lowest among all six metrics being studied. This is not surprising, since SSIM relies on local windowing, point-to-point cross correlation, and only examines in the spatial

domain. As an extension to SSIM, CW-SSIM has access to more abundant spectral-spatial information due to the steerable pyramid decomposition. As a result, the CW-SSIM performance improves significantly over SSIM. However, the performance is still not satisfactory with the low precisions (P@1=0.67 and MAP=0.72). The performance with STSIM-1 is much more encouraging, with the two precision values above 0.9 and the MRR value being 0.99. This verifies that seismic images can be appropriately characterized as texture images.

As to the DM metric we developed in this work, although it is not adequate yet to serve as an independent seismic similarity metric in its current preliminary form, it obviously helps when combined with others. As demonstrated in Table I, DM combined with CW-SSIM yields much improved precisions (P@1 increases from 0.67 to 0.92, while MAP from 0.72 to 0.82). Moreover, DM combined with STSIM-1 further enhances the retrieval performance over STSIM-1. Being the best metric over all, STSIM-1+DM (or SeiSIM) yields perfect values for P@1 and MRR, and is near perfect when MAP is concerned. We believe that such significant improvement is due to the introduction of geological attributes through DM. Figure 6 compares the similarity scores generated in two typical retrieval experiments. In both experiments, STSIM-1 and STSIM-1+DM generate much higher scores for the matching images. Moreover, STSIM-1+DM scores are more consistent within each image group, which is desirable for the application of interest.

IV. Conclusion

In this paper, we explored structural similarity evaluation for retrieval of seismic data, specifically in the form of 2-D survey maps. We first developed a geological similarity metric, DM, which is based on structural information extracted from discontinuity maps. By further combining DM with a texture similarity metric (STSIM-1), we obtained a structural seismic similarity metric (SeiSIM). Our preliminary experiments with a small database yielded excellent results, indicating that the strategy of integrating texture and geological characteristics is very promising for the intended seismic similarity evaluation.

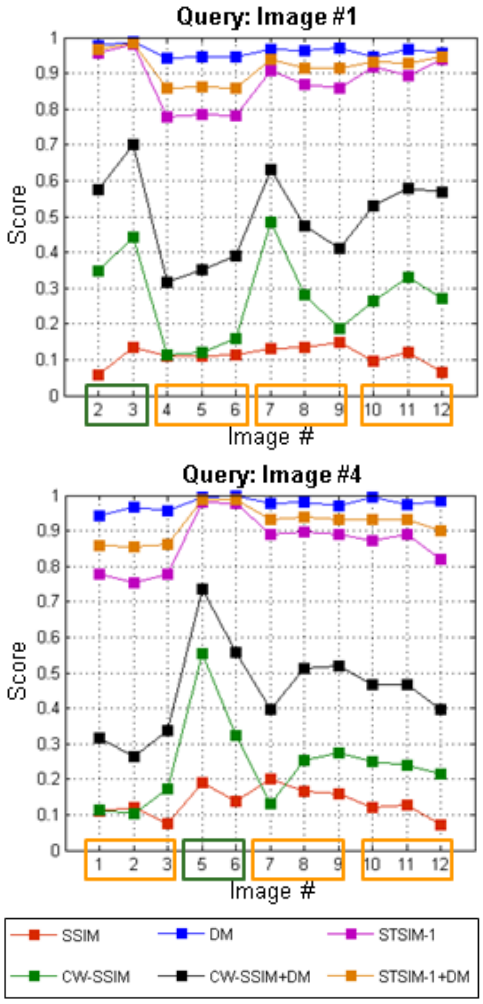

Fig. 6. Comparison of similarity scores generated in two typical retrieval experiments. Here, images 1-3 belong to the group of horizons; images 4-6 belong to the group of salts; images 7-9 belong to the group of faults; and images 10-12 belong to the group of noisy horizons.

Acknowledgment

This work is supported by the Center for Energy and Geo Processing (CeGP) at Georgia Tech and by King Fahd University of Petroleum and Minerals (KFUPM). Mr. Hasan Al-Marzouqi at CeGP prepared the database for the experiments.

References

[1] G. H. Lee, H. J. Kim, D. C. Kim, B. Y. Yi, S. M. Nam, B. K. Khim, and M. S. Lim, "The acoustic diversity of the seabed based on the similarity index computed from chirp seismic data." *ICES Journal of Marine Science / Journal du Conseil*, vol. 66, no. 2, pp. 227 – 236, 2009.

[2] M. Chiodi, G. Adelfio, A. DAlessandro, and D. Luzio, "Clustering and registration of multidimensional functional data," in *Statistical Models for Data Analysis*, ser. Studies in Classification, Data Analysis, and Knowledge Organization, P. Giudici, S. Ingrassia, and M. Vichi, Eds. Springer International Publishing, 2013, pp. 89–97.

[3] M. Vyas and A. Sharma, "Systems and methods for optimal stacking of seismic data," Oct. 31 2013, uS Patent App. 13/855,783. [Online]. Available: http://www.google.com/patents/US20130286782

[4] Z. Wang, A. C. Bovik, H. R. Sheikh, and E. P. Simoncelli, "Image quality assessment: From error visibility to structural similarity," *Image Processing, IEEE Transactions on*, vol. 13, no. 4, pp. 600–612, 2004.

[5] T. Pappas, D. Neuhoff, H. de Ridder, and J. Zujovic, "Image analysis: Focus on texture similarity," *Proceedings of the IEEE*, vol. 101, no. 9, pp. 2044–2057, Sept 2013.

[6] Z. Wang, E. P. Simoncelli, and A. C. Bovik, "Multi-scale structural similarity for image quality assessment," in *IEEE Asilomar Conference on Signals, Systems and Computers*, 2003.

[7] Z. Wang and E. P. Simoncelli, "Translation insensitive image similarity in complex wavelet domain," in *IEEE International Conference on Acoustics, Speech and Signal Processing*, 2005.

[8] Z. Wang and Q. Li, "Information content weighting for perceptual image quality assessment," *Image Processing, IEEE Transactions on*, vol. 20, no. 5, pp. 1185–1198, 2011.

[9] J. Zujovic, T. Pappas, and D. Neuhoff, "Structural texture similarity metrics for image analysis and retrieval," *Image Processing, IEEE Transactions on*, vol. 22, no. 7, pp. 2545–2558, July 2013.

[10] E. Simoncelli, W. Freeman, E. Adelson, and D. Heeger, "Shiftable multiscale transforms," *Information Theory, IEEE Transactions on*, vol. 38, no. 2, pp. 587–607, March 1992.

[11] K. J. Marfurt, V. Sudhaker, A. Gersztenkorn, K. D. Crawford, and S. E. Nissen, "Coherency calculations in the presence of structural dip," *Geophysics*, vol. 64, no. 1, pp. 104–111, 1999.